PART VI

MULTILAYER DESIGNED MATERIALS

CHAPTER 18

Multilayer Coextrusion of Starch/Biopolyester

L. AVÉROUS

ECPM-LIPHT (UMR CNRS 7165), University Louis Pasteur, Strasbourg France

18.1 INTRODUCTION

Advanced technology in petrochemical polymers has brought many benefits to mankind. However, it is becoming increasingly obvious that the ecosystem is considerably disturbed and damaged as a result of the use of nondegradable materials for disposable items. The environmental impact of persistent plastic wastes is becoming a global concern, and alternative disposal methods are not unlimited. Besides this,

Biodegradable Polymer Blends and Composites from Renewable Resources. Edited by Long Yu

petroleum resources are finite and approaching depletion. It is becoming important to find plastic substitutes based on sustainability, especially for short-term packaging and disposable applications. Starch may offer a substitute for petroleum-based plastics. Starch is a renewable and degradable carbohydrate and can be obtained from various botanical sources (wheat, maize, potato, and others). Starch, by itself, has severe limitations due to its water sensitivity (Rouilly and Rigal, 2002). Articles made from starch swell and deform upon exposure to moisture. In recent decades, several authors (Tomka, 1991; Swanson, 1993; Avérous, 2004) have shown the possibility of transforming native starch into thermoplastic resinlike products under destructuring and plasticizing conditions. Unfortunately, plasticized starch, also called "thermoplastic starch," is a very hydrophilic material with limited performance. One way to overcome these difficulties and to maintain its biodegradability consists of associating plasticized starch with another biodegradable polymer (Avérous, 2004). Biodegradable polymers show a large range of properties and they can now compete with nonbiodegradable thermoplastics in various fields (packaging, textiles, biomedical, among others) (Van de Velde and Kiekens, 2002; Steinbuchel, 2003). Avérous has proposed a tentative classification of these biodegradable polymers in two main groups and four different families (Avérous, 2004). The main groups are (i) agropolymers (polysaccharides, proteins, etc.) and (ii) biopolyesters (biodegradable polyesters) such as poly(ester amide) (PEA), poly(lactic acid) (PLA), poly(ε-caprolactone) (PCL), poly(hydroxyalkanoate) (PHA), and aromatic and aliphatic copolyesters (Avérous, 2004).

Melt blending is one established method for associating different polymers. Plasticized starch (PLS) has been blended with various biodegradable polyesters, such as PCL (Huang et al., 1993; Bastioli et al., 1995; Koenig and Huang, 1995; Narayan and Krishnan, 1995; Pranamuda et al., 1996; Amass et al., 1998; Myllymäki et al., 1998; Vikman et al., 1999; Avérous et al., 2000b; Matzinos et al., 2002; Schwach and Avérous, 2004), PLA (Martin and Avérous, 2001; Schwach and Avérous, 2004; Huneault and Li, 2007), PHA (Huang et al., 1993; Ramsay et al., 1993; Koenig and Huang, 1995; Verhoogt et al., 1995), poly(butylene succinate-*co*-butylene adipate) (PBSA) (Ratto et al., 1999; Avérous and Fringant, 2001; Schwach and Avérous, 2004), poly(butylene adipate-*co*-butylene terephthalate) (PBAT) (Avérous and Fringant, 2001), and PEA (Avérous et al., 2000b; Schwach and Avérous, 2004). Blending PLS with these biopolyesters resulted in a significant improvement of the properties of plasticized starch. However, although a "protective" polyester skin layer was formed at the surface of some blends under certain conditions, for instance during injection molding or extrusion (Belard et al., 2005), the moisture sensitivity of PLS was not fully addressed. In an effort to develop starch-based applications, coating the starchy material with hydrophobic (compared to PLS) and biodegradable polyester layers would be preferred.

Multilayer coextrusion has been widely used in the past decades to combine the properties of two or more polymers into a single multilayered structure (Schrenk and Alfrey, 1978; Han, 1981). Some studies have reported the use of plasticized starch and biopolyesters in coextrusion (Avérous et al., 1999; Wang et al., 2000; Martin et al., 2001; Martin and Avérous, 2002; Schwach and Avérous, 2004).

Other techniques may be used for the preparation of starch-based multilayers, such as compression molding (Van Soest et al., 1996; Hulleman et al., 1998; Hulleman et al., 1999; Martin et al., 2001; Schwach and Avérous, 2004). Coating is also mentioned in the literature; coating has been achieved by spraying (Shogren and Lawton, 1998) or painting (Lawton, 1997) different dilute liquids such as biopolyester solutions onto the starch-based material. Nevertheless, coextrusion appears to be the best option since it offers the advantages of being a one-step, continuous, and versatile process. Realistic development of moisture-resistant starch-based products is attempted through multilayer coextrusion, allowing the preparation of sandwich-type structures with PLS as the central layer and the hydrophobic component as the surface outer layers.

However, there are some inherent problems with the multiphasic nature of the flow during coextrusion operations, such as nonuniform layer distribution, encapsulation, and interfacial instabilities, which are critical since they directly affect the quality and functionality of the multilayer products. There has been extensive experimental and theoretical investigation of these phenomena (Dooley, 2005). The layer encapsulation phenomenon corresponds to the surrounding of the more viscous polymer by the less viscous one (Lee and White, 1974). Experimental investigations on the shape of the interface have been reported (Southern and Ballman, 1973; Khan and Han, 1976) showing that viscosity differentials between respective layers dominate over elasticity ratios. Conversely, White et al. (1972) reported the influence of normal stress differences on the shape of the interface. In more recent experimental studies, Dooley and co-workers (Dooley and Stout, 1991; Dooley et al., 1998) investigated the layer rearrangement during coextrusion, and the importance of the channel geometry. They indicated that coextrusion of identical polymers (i.e., with matched viscosities) can lead to layer rearrangement, due to the die geometry.

Yih and Hickox (Yih, 1967; Hickox, 1971) pioneered studies on interfacial instabilities, suggesting that viscosity differences may cause instabilities of stratified flow. Schrenk and co-workers (Schrenk and Alfrey, 1978; Schrenck et al., 1978) investigated the factors responsible for the onset of instabilities, and suggested the existence of a critical shear stress value beyond which interfacial instabilities are likely to occur. Han and Shetty (1976, 1978) described in detail the factors responsible for the occurrence of instabilities, such as critical shear stress at the interface, viscosity and elasticity ratio, and layer thickness ratio. In addition, many authors (Sornberger et al., 1986a,b; Karagiannis et al., 1988; Khomani, 1990a,b; Su and Khomani, 1992a,b; Wilson and Khomani, 1992; Wilson Khomani, 1993; Gifford, 1997; Tzoganakis and Perdikoulias, 2000; Dooley, 2005) have modeled multilayer flows by computer simulation, and attempted to elucidate the influence of viscoelasticity, layer thickness, and die geometry on layer rearrangements and onset of instabilities. Karagiannis et al. (1988) modeled encapsulation phenomenon, and Sornberger and co-workers (Sornberger et al., 1986b) studied the interface position in two-layer flat film coextrusion. In a later work, Gifford (1997) attempted to account for the effects of viscoelasticity on the layer deformation. Most numerical investigations only partly addressed the layer uniformity problem, due to the complexity of the stratified flow systems. Khomani and co-workers (Khomani, 1990a; Su and Khomani,

1992a,b; Wilson and Khomani, 1992; Wilson and Khomani, 1993) contributed significantly to the understanding of the onset and propagation of interfacial instabilities and of interface deformations, thanks to a specially designed optical interface monitoring system allowing visualization, after image reconstruction, of the multilayer flow in the die. Khomani and Su (Khomani, 1990a; Su and Khomani, 1992a,b) examined the effects of elasticity and viscosity on the interfacial stability, according to the die geometry and layer depth ratio. They determined the role of elasticity in the mechanism of instabilities. Wilson and Komani (1992, 1993) studied experimentally and numerically the propagation of periodic flow disturbances, and determined the stable and unstable flow conditions, with a good agreement with models. In a more recent study, Tzoganakis and Perdikoulias (2000) studied experimentally the effects of material properties and flow geometry on the appearance of interfacial instability.

Despite the number and diversity of studies on multilayer flows and stability, only few articles (Avérous et al., 1999; Martin and Avérous, 2002; Wang et al., 2000; Martin et al., 2001; Schwach and Avérous, 2004) have reported the use of plasticized starch and polyester in coextrusion processes. Different stratified structures were processed by coextrusion and studied with PCL (Wang et al., 2000; Martin et al., 2001; Schwach and Avérous, 2004), PBSA (Wang et al., 2000; Martin et al., 2001; Schwach and Avérous, 2004), PEA (Wang et al., 2000; Martin et al., 2001; Martin and Avérous, 2002; Schwach and Avérous, 2004), PLA (Wang et al., 2000; Martin et al., 2001; Schwach and Avérous, 2004), polybutylene adipate-*co*-butylene terephthalate (PBAT) (Wang et al., 2000; Schwach and Avérous, 2004), or polyhydroxybutyrate-*co*-hydroxyvalerate (PHBV) (Avérous et al., 1999), a biopolyester which belong to the PHA family.

18.2 MATERIALS AND PROCESS

18.2.1 Materials

Native wheat starch was purchased from Chamtor (France). The starch contains 74% amylopectin and 26% amylose, with residual protein and lipid contents less than 0.2% and 0.7%, respectively. Glycerol of 99.5 % purity was used as a nonvolatile plasticizer. Various types of PLS (PLS1, PLS2, and PLS3) were prepared, differing in the glycerol:starch ratio and the water content. Table 18-1 shows the different PLS formulations prepared (with starch, water, and glycerol contents before and after extrusion) and some resulting properties. Both powdery and extruded products were used in the study for the coextrusion process. Most PLS properties and mechanical behavior have been given in previous publications (Avérous, 2004).

The aliphatic poly(ester amide) (PEA) LP BAK 404 was kindly supplied by Bayer AG (Germany). The poly(ε-caprolactone) (PCL) CAPA 680 was purchased from Solvay (Belgium). The poly(lactic acid) (PLA), 92% L-lactide and 8% *meso*-lactide, was obtained from Cargill (USA). The poly(butylene succinate-*co*-butylene adipate) (PBSA) Bionolle 3000 was obtained from Showa Highpolymer Co. (Japan). Finally, PHBV (Biopol D600G, 12% HV) was kindly supplied by

TABLE 18-1 Characteristics of Different Biopolyesters

	PLA Cargill Nature Works	PHBV Monsanto Biopol D600G	PBSA Showa Bionolle 3000	PEA Bayer BAK 1095	PCL Solway CAPA 680
MW (g/mol)	150,000[a]	430,000[a]	234,000[b]	37,000[c]	80,000[a]
Density	125	125	123	107	111
Melting point (°C DSC)	158	144	114	112	65
Glass transition (°C DSC)	58	−1	−45	−29	−61
Modulus (MPa)	2050	500	249	262	190
Elongation at break (%)	9	20–30	>500	420	>500
Water permeability[d] (g/m^2/day) at 25°C	172	21	330 with 7% HV	680	177

[a]Data obtained from the provider.
[b]*Source*: He et al. (2000).
[c]*Source*: Krook et al. (2005).
[d]*Source*: Shogren (1997).

Monsanto (USA). For some coextrusion experiments, LDPE (Lacqtene 1070MG24, Arkema, France) was used, as a model.

18.2.2 Processing and Procedures

Plasticized Starch Preparation The first step of the process consists of preparing plasticized wheat starch (PLS). Native wheat starch was introduced into a turbomixer. Glycerol and water were then added slowly under stirring according to the formulation (Table 18-2). After complete glycerol addition, the mixture was mixed at high speed to obtain a homogeneous dispersion. The mixture was placed in a vented oven at 160°C for 20 min and stirred to allow vaporization of water and diffusion of glycerol into the starch granules, and finally this dry blend was placed again in the oven for 20 min.

TABLE 18-2 Plasticized Starch Formulations

Formulation	Starch Content (wt%)	Glycerol Content[a] (wt%) GC	Glycerol/ Starch Ratio[a] G/S	Moisture Content[a] (wt%) MC	Density	Glass Transition (°C) T_g
PLS1	74	10 (11)	0.14 (0.14)	16 (8.5)	1.39	43
PLS2	70	18 (18)	0.26 (0.25)	12 (8.7)	1.37	8
PLS3	65	35 (30)	0.54 (0.50)	0 (12.6)	1.34	−20

[a]Compositions are given in wt% total wet basis, and values in parentheses are the glycerol or moisture contents, or glycerol/starch ratio after extrusion at 105°C and equilibration at 23°C, 50% RH.

For coextrusion process, starch can be introduced as a powder (dry blend) or as granules. In the latter case, the dry blend is extruded, granulated after air-cooling, and then equilibrated at a given relative humidity and temperature.

Coextrusion Procedure Figure 18-1 presents a schematic view and photograph of the experimental set-up for the coextrusion, which consists of two single-screw extruders, a feedblock attached to a wide, flat die, and a three-roll calendering system. The PLS extrusion step was based on a single-screw extruder (SCAMIA S 2032, France), equipped with a conical-shaped element to provide high shearing with a 20 mm screw diameter and an L/D ratio of 11. A 30 mm diameter, 26 : 1 L/D single screw extruder was used for the cap layer. Figure 18-2 presents a

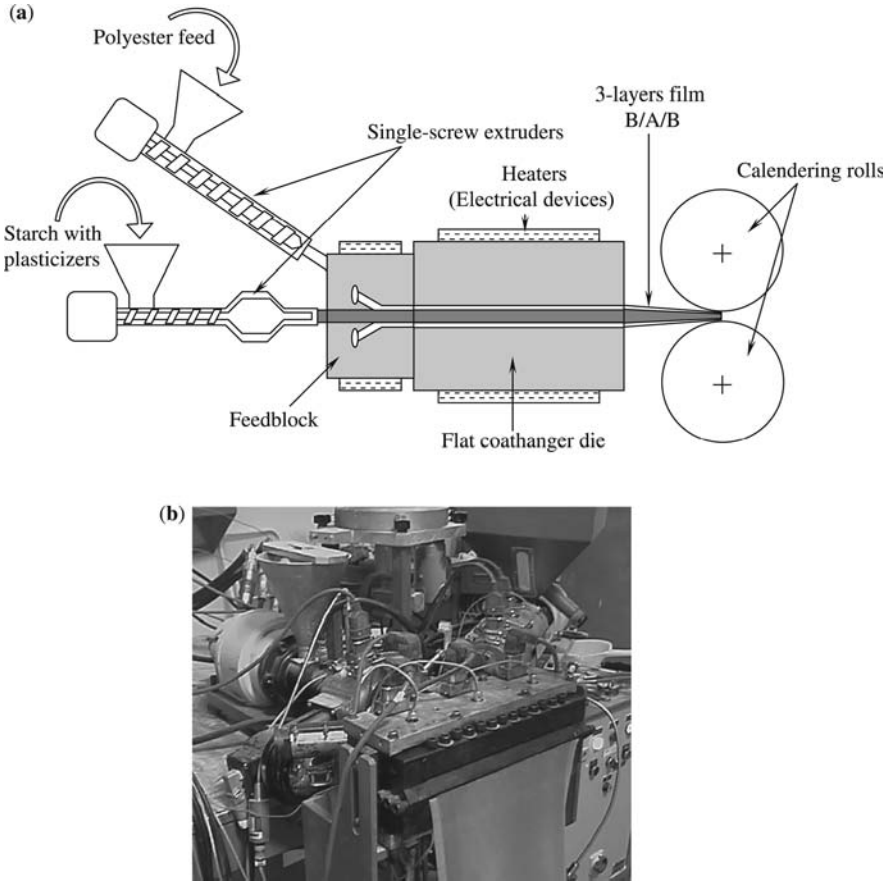

Fig. 18-1 (a) Schematic illustration of the coextrusion system; (b) photograph of the experimental set-up without the three-roll calendaring system on the right side; the mono-extruder is for biopolyester feed.

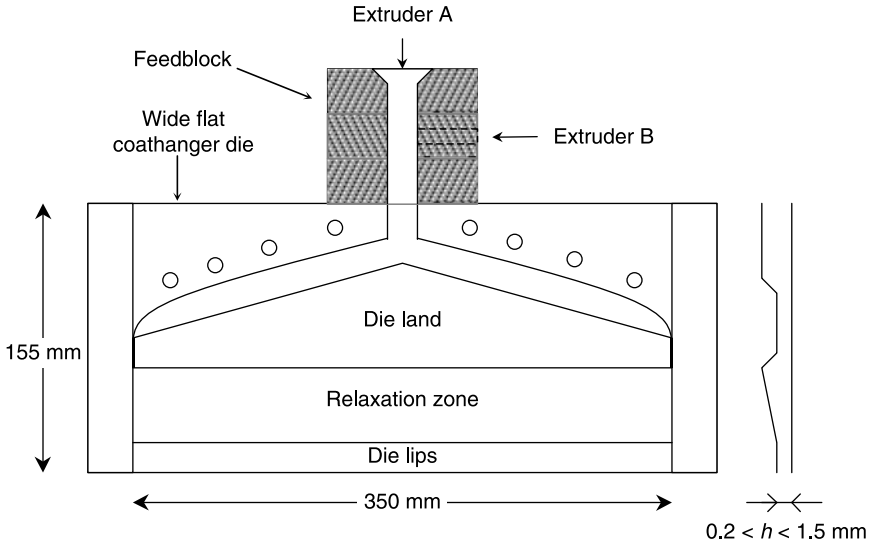

Fig. 18-2 Schematic view of the feedblock and flat coathanger die. The feedblock consists of three different modules: (i) the manifold module, (ii) the feed-port module, and (iii) the transition module.

schematic view of a flat coathanger die with the feedblock attachment. The die is constituted by a rectangular entry channel ($L \times W \times h = 50\,\text{mm} \times 30\,\text{mm} \times 4\,\text{mm}$), a coathanger of decreasing cross-section, a die land area of adjustable height, a relaxation area of decreasing thickness (from 4.5 to 1 mm), and finally the die lips ($L = 350\,\text{mm}$). Figure 18-3 shows a schematic of the feedblock, allowing

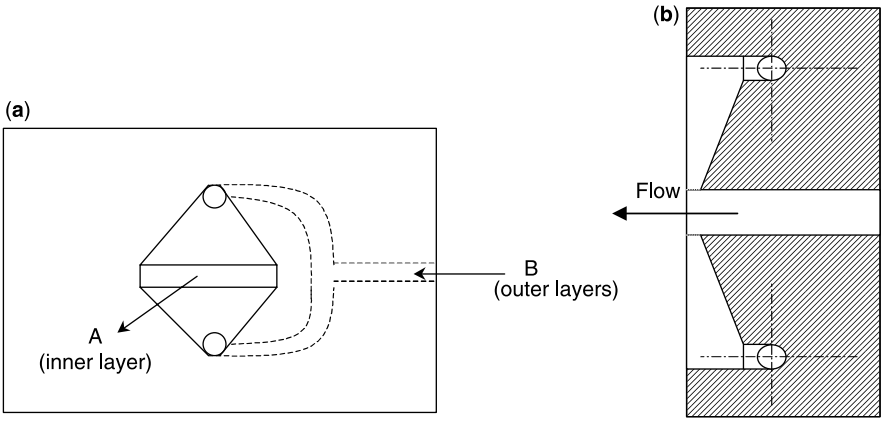

Fig. 18-3 Front view (a) and transverse cross-section (b) of the middle block of the feedblock. The rectangular flow channel of the feedblock is $W \times L \times h = 30\,\text{mm} \times 120\,\text{mm} \times 4\,\text{mm}$ and the side stream inlet tube diameter is 8 mm.

the polymer melt from each extruder to be combined into a stratified three-layer melt stream. The feedblock was designed to receive two feed streams, and the slit section has the dimensions length 120 mm, width 30 mm, and thickness 4 mm. As may be seen from Fig. 18-2, the three blocks are put together to form the feedblock. The melt stream forming the outer layers (from the polyester extruder) is split in half along two flow paths (Fig. 18-3a) and then merges with the main stream (inner layer, from the PLS extruder) in the slit section, 30 mm before the flat die entry. From the die inlet, the multilayer melt streams may flow through the die inlet and spread uniformly across the entire width of the die. The spreading of the three-layer flow across the die is due to the coathanger geometry, that is, restriction of the channel section along the flow direction. The die land area (Fig. 18-2), whose section is determined by a restriction bar, is adjustable in height by changing the thickness of the movable restriction bar. The die land channel height could be varied from 1.5 mm to 4 mm. Consequently, the flow path profile along the axial direction can be modulated from distorted to relatively smooth.

In routine experiments, the coextrusion line was run for at least 30 min to ensure steady-state operation. Initially, the flow rates of all polymers used were measured independently for each extruder, at the corresponding screw speeds, so that the A : B flow ratio could be controlled. In all experiments, the outer layer was always the minor component. After exiting the die, the coextruded film was cooled with the chill roll, and collected to analyze the wavy instabilities (magnitude and periodicity). A cooling air jet was applied to the film exiting the die in some cases, especially when the higher moisture content PLS was used, to prevent material expansion by water vaporization at the exit.

The flow rates of the polymers used were measured independently for each extruder, at the corresponding screw speeds, so that the PLS/polyester flow ratio could be controlled. In all experiments, the outer layers constituted the minor component, for cost efficiency reasons. PLS was processed within a temperature range of 100–130°C, and the outer layer polyesters were processed at 110°C, 120°C, 140°C, 160°C, and 180°C for PCL, PBSA, PEA, PLA, and PHBV, respectively. Because melt temperature differentials between respective layers should not be too great (Mitsoulis, 1988), the PLA had to be plasticized to lower its processing temperature. The effect of various plasticizers on the thermal properties of PLA has been reported previously (Martin and Avérous, 2001). In addition, a low-melting-temperature PHBV grade was used with Biopol D600G, which has a high HV content. Once the steady-state conditions were reached, the multilayer films were collected and set apart for further analyses.

18.3 CHARACTERIZATION

18.3.1 Peel Test

Peel tests were carried out on a Thwing-Albert peel tester (model 225-100) at a rate of 50 mm/min. The test specimens were conditioned at 23°C and 50% RH, and cut from

the multilayer films into 100 mm × 20 mm strips prior testing. The outer polyester layer was delaminated manually and gripped onto the load cell, while the film was secured on a sliding plate, so that a constant 90° angle between the polyester layer and PLS was maintained during the test. Load data collection started after 3 seconds of pre-peel. A mean value was determined from each test, and each sample was tested 5 times.

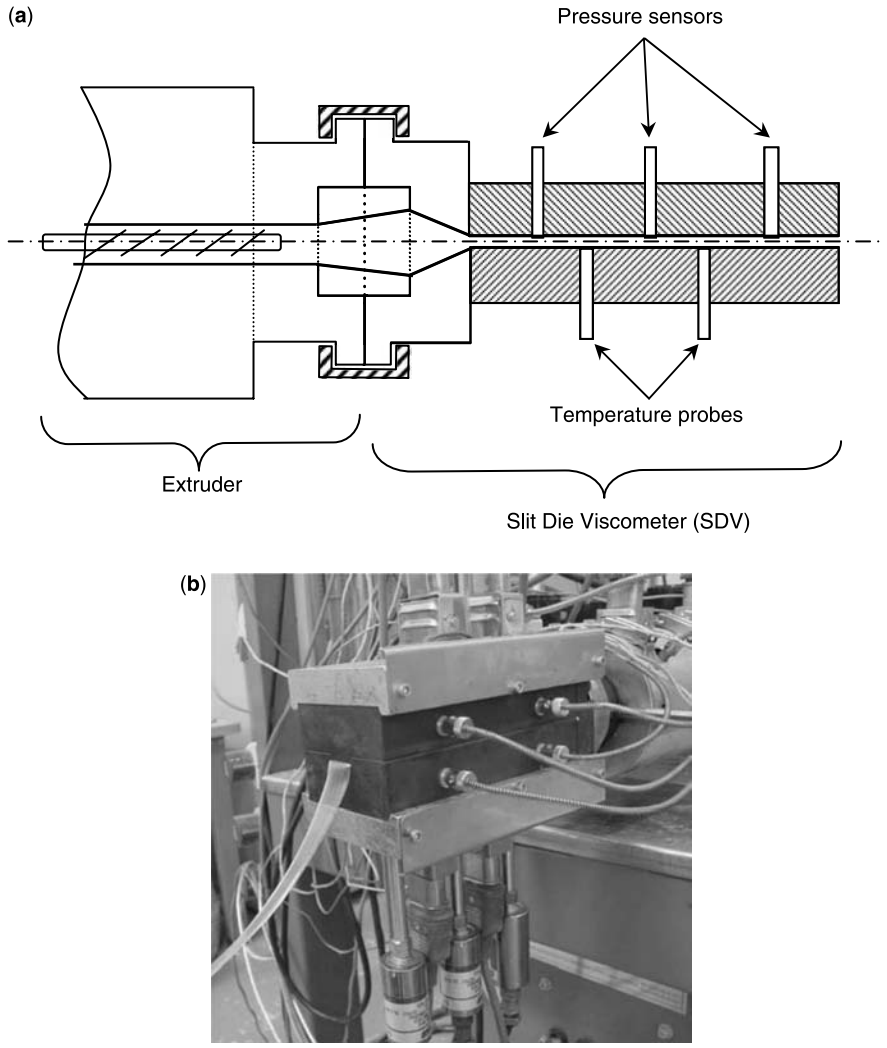

Fig. 18-4 (a) Schematic illustration of the in-line SDV rheometer; (b) photograph of the SDV system.

18.3.2 Surface Tension

A Krüss G23 goniometer (Germany) was used to measure the contact angle and to capture the kinetics of sorption (slope of the curve contact angle as a function of time) in relation to the material's hydrophobic character.

18.3.3 Optical Microscopy

A Leica transmission optical microscope was used to capture the shape of the interface between the respective layers of coextruded structures. Each film was either freeze-fractured, or cut with a diamond-like precision saw. The PLS phase was tinted with iodine vapor to better differentiate layers.

18.3.4 Melt Rheology

The viscosity of all products used in coextrusion experiments was measured using a specially designed slit die viscometer (SDV) as illustrated in Fig. 18-4. The use of this system was fully described in a previous publication (Martin et al., 2003). Shear rates in the range of $1-1000\,s^{-1}$ were obtained. PLS materials were tested in both powdery and pellet forms. To analyze the behavior of the multilayer materials, the SDV was associated with the feedblock, at the exit.

18.4 RESULTS AND DISCUSSION

18.4.1 Effect of Process Parameters: Melt-State Behavior

This part is more particularly focused on the analysis of the coextrusion of poly(ester amide) and plasticized starch. Because of the complexity of multilayer flows, attention will be paid to the rheological behavior of each component, the effects of operating conditions and viscosity ratios on the layer uniformity, and the mechanisms giving rise to instabilities at the interface.

Rheological Behavior of Neat Components Table 18-3 presents the physical characteristics and rheological parameters of the different materials used in

TABLE 18-3 Rheological Parameters

Material	E/R (K)	Ko Consistency[a] (Pa s)^m
PEA	3360	9,920
LDPE	1960	9,000
PLS1	4500	19,300
PLS2	5860	12,600
PLS3	5860	10,350

[a] m = pseudoplasticity index.

this section. The viscosities were measured using the specially designed slit die viscometer at the exit of the extruder (see Fig. 18-4). The rheological properties of PEA and PLS3 products are presented in Fig. 18-5. The viscosity values of all PLS products (both powder and pellet types), determined using the SDV, are fully presented in a previous article (Martin et al., 2003). Depending on the temperature range, melt PEA viscosities lay around that of molten PLS. Melt viscosity ratios between PLS and PEA ranging from 1 to 5 could thus be obtained, by control of the process temperatures of the respective polymers. It should be noted that PEA melt temperature below 150°C could not be obtained; otherwise, some fluctuations of the extruder torque occur. Unsteady torque at given screw speed is known to cause flow disturbances due to pressure variations and to promote interfacial instabilities (Khomani, 1990a; Su and Khomani, 1992a,b; Wilson and Khomani, 1992) (see Fig. 18-6).

Interface Deformation and Encapsulation Experiments were carried out without any die to check whether the three layers were evenly distributed and were uniform in thickness at the feedblock exit. Extrusion grade LDPE was used in both extruders to perform these trials. To distinguish the interface between respective layers, the central layer and the cap layers were pigmented in black and white, respectively. Uniform layer distribution and flat interfaces are obtained when the LDPE streams have similar temperatures. However, when a melt differential as low as 20°C was imposed, the outer layers started to surround the central layer, along the 30 mm flow length (from the merging point to the feedblock exit). This configuration, consisting of a higher melt temperature and lower viscosity polymer as the cap layers, was chosen to closely reflect the conditions of PLS/polyester coextrusion. In effect, the temperature processing range of PLS is limited and starch melt viscosity is generally higher than that of PEA. The layer rearrangement observed, where the less viscous outer layers start to surround the other layer, is called "encapsulation." The encapsulation of the more viscous layer by the less viscous one is a well-known phenomenon, and has been extensively dealt with in the literature (Dooley, 2005). Other authors (Southern and Ballman, 1973; Lee and White, 1974) have shown that when the viscosity ratio increases, the degree of encapsulation increases accordingly. The interface shape change is explained by viscous encapsulation, in which layers rearrange themselves to minimize the total energy. The encapsulation effects may be decreased by reducing the viscosity difference between the layers.

However, the viscosity difference is not the only factor inducing encapsulation. The shape and length of the flow channel also have a nonnegligible influence. When the above three-layer systsem was passed through the feedblock associated with the SDV, some degree of encapsulation was found at the exit of the SDV with a viscosity ratio close to unity. The cap layers in contact with the die wall are exposed to higher shear stresses and greater heat dissipation than the central layer, resulting in a progressive viscosity evolution. A specific geometric design of the flow channel should compensate for these effects (Dooley, 2005).

When PLS and PEA were coextruded together, the PEA cap layers almost encapsulated the central layer, whatever the flow conditions. The cap component commonly encapsulated the central layer at the side wall of the die. The degree of

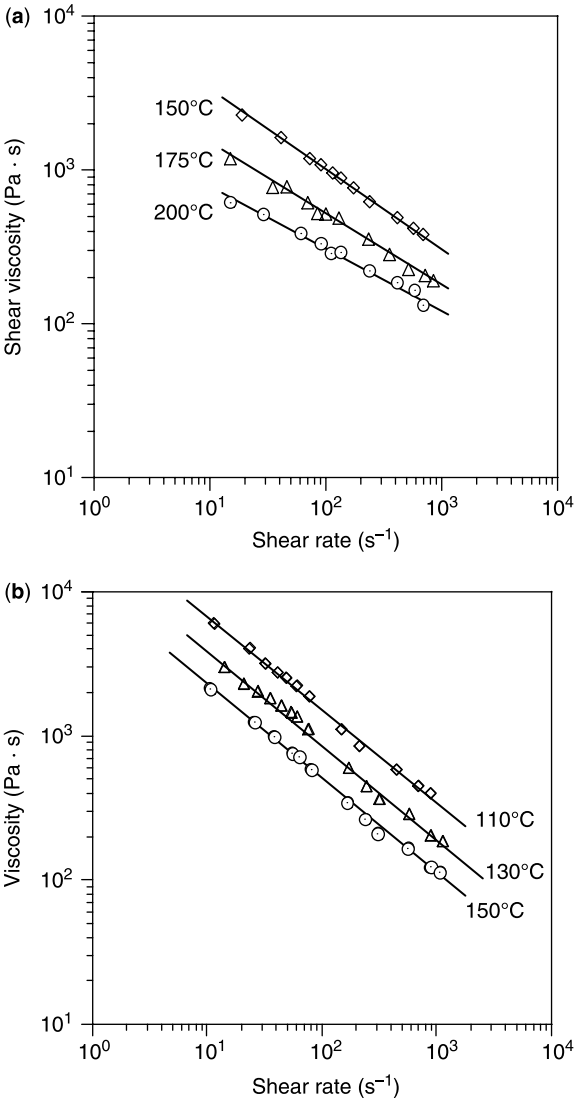

Fig. 18-5 Rheological properties of (a) PLS3 and (b) PEA at various temperatures. Source: Martin and Avérous (2002).

encapsulation, referred to the percentage area surrounded by the outer layers, ranged from partial (0–50%) to total (100%) in the film-forming die. Decreasing the cap layer flow rate usually resulted in a decrease of the extent of encapsulation on the edges of film, from 10–15 mm down to 2–4 mm. But the occurrence of encapsulation was not thought to be very critical in this case since it commonly affects the edges of the coextruded structures only, which are usually discarded.

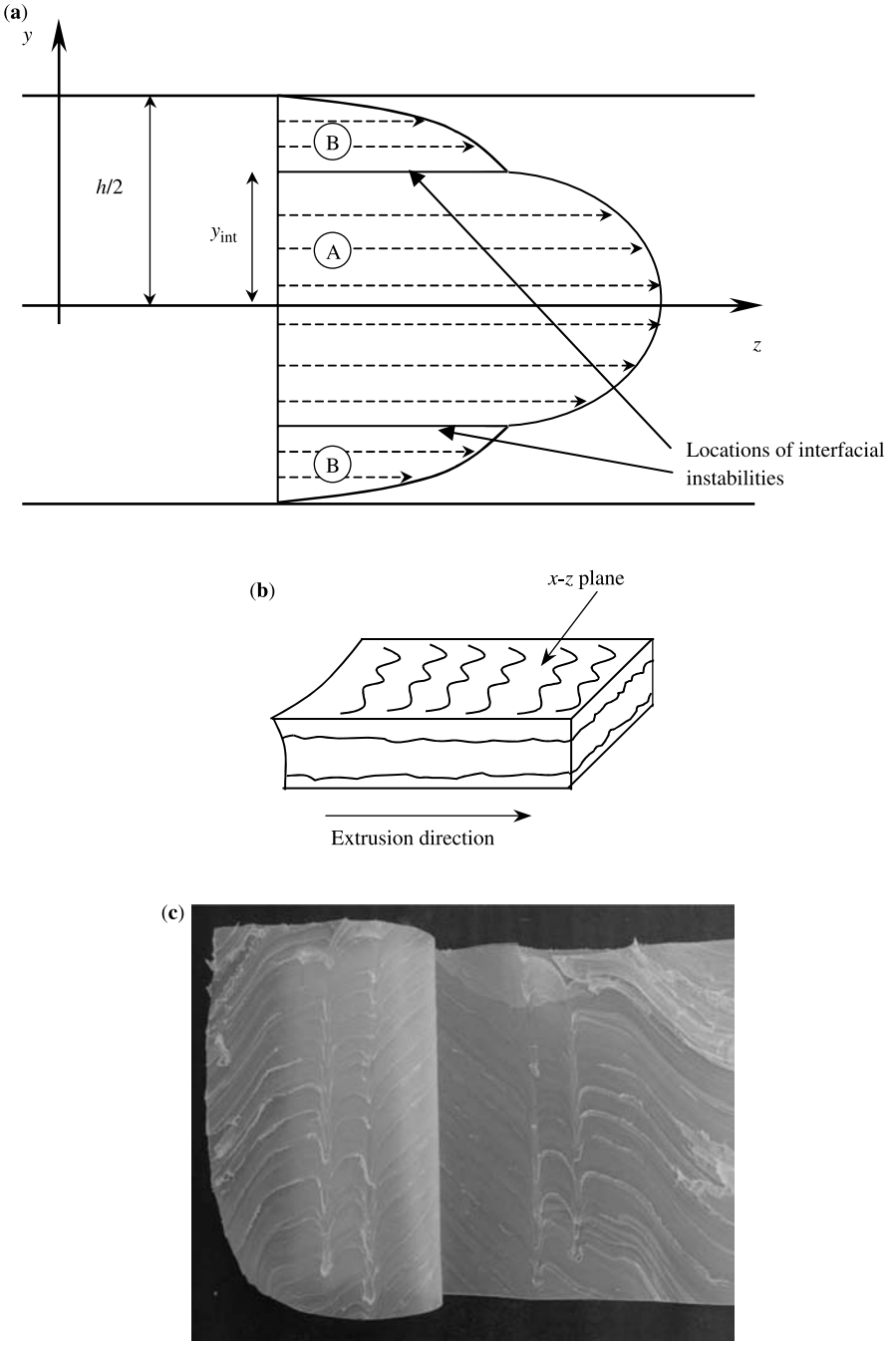

Fig. 18-6 (a) Velocity profile of a three-layer B/A/B through parallel plates; (b) schematic of a multilayer film exhibiting wavy instabilities at the interfaces; (c) photograph of a coextruded and delaminated film exhibiting wavelike instabilities.

Interfacial Instability Unlike encapsulation effects, the occurrence of interfacial instabilities is very critical because it directly affects the quality and functionality of the coextruded films (Dooley, 2005). Figure 18-6a is an illustration of the velocity profile of a three-layer flow through a slit die of gap $y = h$. Owing to the symmetry, only one half of the channel height is considered. Under stable flow conditions, the interfaces of the final multilayer film may be flat and smooth. Conversely, interfacial instabilities manifest themselves as wavelike distortions of the interface between two polymers across the width of the film, as shown by the schematic (Fig. 18-6b) and the photograph (Fig. 18-6c).

In the system studied, consisting of shear-thinning polymers in simple shear flow, several mechanisms can give rise to interfacial instabilities. According to our experimental results, interfacial instability set in within the die. The variables known to play a important role in the occurrence of instabilities are the skin-layer viscosity, the layer thickness ratio, the total extrusion rate, and the die gap. Moreover, interfacial instabilities are known to result when a certain shear stress value at the interface of two polymers is exceeded. The onset of interfacial instabilities can thus be characterized by the critical interfacial shear stress (CISS). The interfacial shear stress τ_{int} can be calculated from the known coextrusion conditions and the flow characteristics by equation (18.1) where τ_w is the shear stress at the die wall (at $y = h/2$), y_{int} is the position of the interface, and h is the slit thickness.

$$\tau_{int} = \frac{\tau_w \cdot y_{int}}{(h/2)} \tag{18.1}$$

The shear stress at the wall is determined by equation (18.2) where $(-dp/dz)$ is the axial pressure gradient measured by the wall normal stress measurement.

$$\tau_w = \frac{(dp/dz)}{(h/2)} \tag{18.2}$$

According to equation (18.1), determining the interface position for a given flow ratio allows one to determine the shear stress at the die wall. To measure the interface positions inside the die, the solidified sprues obtained from different experiments were cut into slices along the flow direction, as presented in Fig. 18-7. In the absence of a direct visualization inside the flow channel, the cross-sections of the sprue allow us to determine the repartition of the layers in the distribution channel, the flow restriction zone, the relaxation zone, and the die lips, respectively. The exact interface position was measured with a binocular. The influence of main variables were investigated, while keeping other conditions constant, and flow conditions from stable to unstable were obtained. At the point of incipient instabilities, the CISS can be calculated thanks to the known flow conditions and equations (18.1) and (18.2).

Effect of Viscosity Ratio and Layer Thickness Ratio PLS (dry-blend) and PEA were coextruded together through the feedblock and wide, flat film die. The conditions for the coextrusion of the PEA/PLS3/PEA three-layer system are reported in

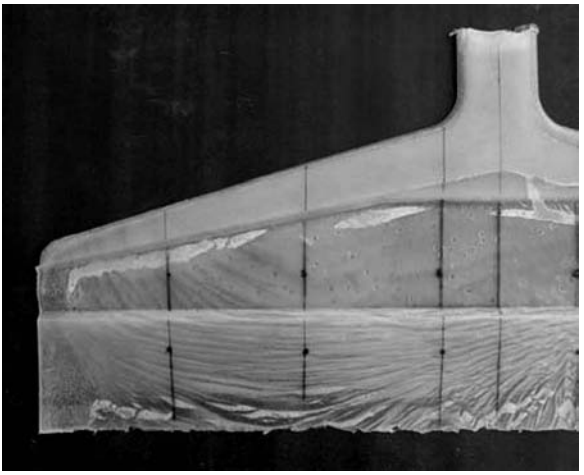

Fig. 18-7 Half-die solidified sprue with incipient instabilities.

Table 18-4. Note that only the total flow rate was measured, and that the individual flow rates were derived from the total flow rate and those determined from corresponding extruder speeds. The total flow rate was maintained in the same range in all experiments, to study the effects of viscosity and thickness ratio only. The flat die temperature was set close to the higher melt temperature layer, so that the

TABLE 18-4 Experimental Coextrusion Conditions of "PEA/PLS3/PEA" 3-Layer System[a]

Test No.	PLS3–Melt Temperature T_{PLS} (°C)	PEA–Melt Temperature T_{PEA} (°C)	Flow-Rate Q_T (g/min)	Thickness Ratio h_{PEA}/h_{PLS}	Interfacial Shear Stress τ (kPa)	Level of Stability
1	110	150	880	0.24	65	Unstable
2	110	150	864	0.38	52	Small instabilities
3	110	150	982	0.58	51	Stable
4	110	150	904	0.79	42	Stable
5	130	150	819	0.26	86	Unstable
6	130	150	870	0.36	90	Unstable
7	130	150	915	0.64	48	Small instabilities
8	130	150	959	0.84	56	Unstable
9	150	150	873	0.27	73	Unstable
10	150	150	902	0.35	64	Unstable
11	150	150	944	0.55	55	Stable
12	150	150	928	0.81	68	Unstable

[a]*Source*: Martin and Avérous (2002).

combined stream did not solidify at the die wall. The interface positions across the entire width of the film at the die exit corresponding to experiments are observed. It may be shown that the interface is not flat, due to some irregular layer distribution. The encapsulation that begins in the feedblock was enhanced by the flow through the die since about 10–15 mm of each edge of film was encapsulated by the cap layers. The coextrusion of the PLS/PEA three-layer system through the wide film die mostly led to unstable flow conditions, even when the viscosity of the respective layers was matched (experiments 5 to 8), and whatever the layer thickness ratio. Note that these trials were carried out with the narrow die gap geometry, that is, a channel height in the die land area as low as 1.5 mm.

Because changing variables like the viscosity of products and the layer thickness ratio did not yield satisfactory results, the combined streams were tested under similar conditions through the SDV instrumented flow channel. We assumed that the locations of interfaces inside the SDV die were equivalent to those at the wide, flat die entry channel, measured from the solidified sprue. As stated previously, the pressure gradient and interface positions allow us to calculate the wall shear stress and the interfacial shear stress. Figure 18-8 shows a plot of the shear stress as a

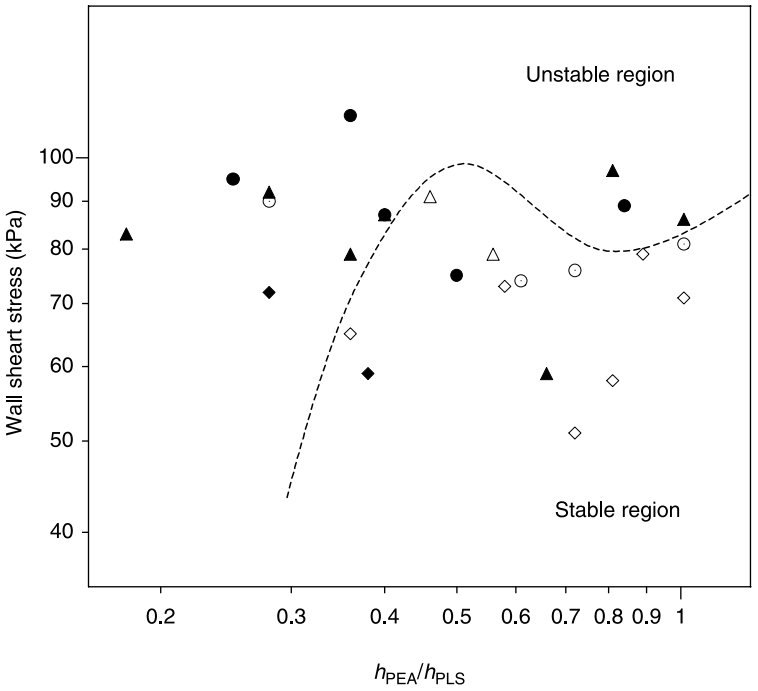

Fig. 18-8 Plot of the wall shear stress versus the layer thickness ratio of "PEA/PLS/PEA" coextruded films: ○, ●, $\eta_B/\eta_A = 1$; △, ▲ $\eta_B/\eta_A = 4$; ◇, ◆ $\eta_B/\eta_A = 0.3$. Filled shapes denote unstable flow regions, whereas white ones represent stable flow conditions. Source: Martin and Avérous (2002).

function of the layer thickness ratio. Despite the scattering of data points, there seems to be a physical limit between stable and unstable regions. In addition, Fig. 18-8 shows that some extent of flow stability may be obtained when the low-viscosity component is the cap layer, with layer ratio between 0.5 and 1 and at moderate wall shear stress. Conversely, low layer thickness ratios or high shear stresses almost exclusively induced instabilities, whatever the viscosity ratio. From these results and the known interface position inside the die, the interfacial shear stress was calculated (Table 18-4). It is clear that higher shear stresses at the interface, due to higher flow rates or lower cap layer thickness, are responsible for the onset of instabilities in the multilayer flow. There seems to be a critical interfacial shear stress (CISS) value above which interfacial instabilities set in, depending on the layer thickness ratio. However, previous studies (Han and Shetty, 1978; Karagiannis et al., 1988; Mavradis and Schroff, 1994) on three-layer films demonstrated that the CISS, for a given polymer system, is independent on the process parameters varied, including layer thickness ratio. For our three-layer system, no such trend of CISS exist, since values at incipient instabilities ranged from 52 to 64 kPa, and because instability-free flows were observed beyond 55 kPa. These results are in apparent contradiction with published ones, probably due to the complexity of the system studied and specificity of the rheological behavior of PLS. It may be concluded from this section that low layer thickness ratio and viscosity differences with the cap layer as the more viscous component promote the onset of instabilities.

Effect of the Extrusion Rate and Die Geometry The extrusion rate refers to the magnitude of the total volumetric flow rate measured at the exit of the die. Enhancing extrusion rates result in increasing pressure gradients, and thus increasing shear stress at the die wall. As shown by Han and Shetty (1978) in coextrusion of films, the shear stress is continuous across the interface. Therefore, higher interfacial shear stresses may be reached at high extrusion rates. Moreover, the height of the slit section of the die land may be varied between 1.5 and 4 mm. A change in the slit section height, before the relaxation zone, is expected to cause a diminution of the global pressure drop across the die, thus reducing the shear stress level.

Experiments were aimed at reducing the shear rate in the die. The flow rates of individual melt streams were accordingly varied to increase the extrusion rate across the flat film die of decreasing slit height. The resulting flow rate Q_T was measured at the die exit and the global pressure drop was recorded. The corresponding data are shown in Table 18-5. The most remarkable result is that no flow stability can be obtained with the narrow die gap geometry (G_1 with $h = 1.5$ mm), whereas some instability-free three-layer films were obtained through the larger die land slit section, principally with the G_3 geometry. Increasing the die temperature to 170°C did not seem to help. In fact, increasing the die land slit section induces significant decrease in the shear stress at the wall and at the interface. For instance, in condition 5, the shear stress ranged from 10^5 to 8×10^3 between the G_1 and the G_3 geometries. However, poor layer distribution resulted from the increase of the slit height. The elimination of interfacial instabilities was achieved at the expense of the uniformity of the product. The magnitude of shear stress change through modulation of the

TABLE 18-5 Effect of Extrusion Rate and Die Geometry on the Stability of Coextrusion Flows, Die Temperature $T_{Die} = 150°C$[a]

Test No.	Total Flow Rate Q_T (g/min)	Global Pressure Drop (MPa)[b]			Flow Stability[c]		
		G_1	G_2	G_3	1	2	3
1	48	4.6	3.1	2.5	s	s	s, bld
2	56	5.1	3.9	3.1	u	s	s, bld
3	65	5.8	5.2	4.0	u	s, bld	s, bld
4	78	6.8	5.8	4.5	u	s, bld	u, bld
5	91	7.8	6.4	4.9	u	u, bld	u, bld
6	112	8.6	7.1	5.5	u	u, bld	u, bld

[a] *Source*: Martin and Avérous (2002).
[b] Subscripts 1, 2, and 3 designate the height of the slit section in die land area of 1.5, 2.5 and 3.5 mm, respectively.
[c] s designates a stable flow; u designates an unstable flow; and bld means "bad layer distribution."

geometry and extrusion rate is significant. Increasing extrusion rates and reducing the flow section both favor the onset of instabilities. These results are in good agreement with previously published ones. One may conclude that the film coextrusion of polymers is a compromise between many factors, and that the influence of each parameter needs to be fully ascertained.

Control of the Instability Amplitude with the Shear Rate Ranjbaran and Khomani (1996) showed that a controlled amount of instability can significantly increase interfacial strength of multilayers, thanks to mechanical interlocking. Wang et al. (2000) also described the possible advantages of instabilities in terms of interfacial bonding increase.

We saw that the occurrence of interfacial instabilities is closely related to the shear stress at the interface. As a result, there may be several ways to increase the instabilities in coextruded film, such as increasing the extrusion rates, lowering the outer layer thickness, or reducing the gap in the die land area. Figure 18-9a shows that the amplitude of wave-instabilities is closely dependent on the shear rate. Figure 18-9b shows a micrograph of the cross-sections of PLS-PEA sprues, giving evidence of the penetration of the PEA layer into the PLS phase. In the micrograph, the dark phase is the PLS (tinted with iodine vapor) and the lighter outer phase is the PEA. The amplitude gradually increased from 10 to 170 μm as the shear rate increased. However, that clear trend was not observed for all coextrusion experiments, in particular when the mechanism giving rise to instabilities was not controlled, such as elasticity difference between layers, die exit phenomenon, or velocity profile difference. Finally, it should be added that the extent and, to a certain degree, the amplitude of interfacial instabilities could be readily controlled, and that the main conditions likely to generate instabilities are known. Under control, these instabilities can generate mechanical interlocking and so increase the interfacial adhesion strength on the coextruded material (Schwach and Avérous, 2004).

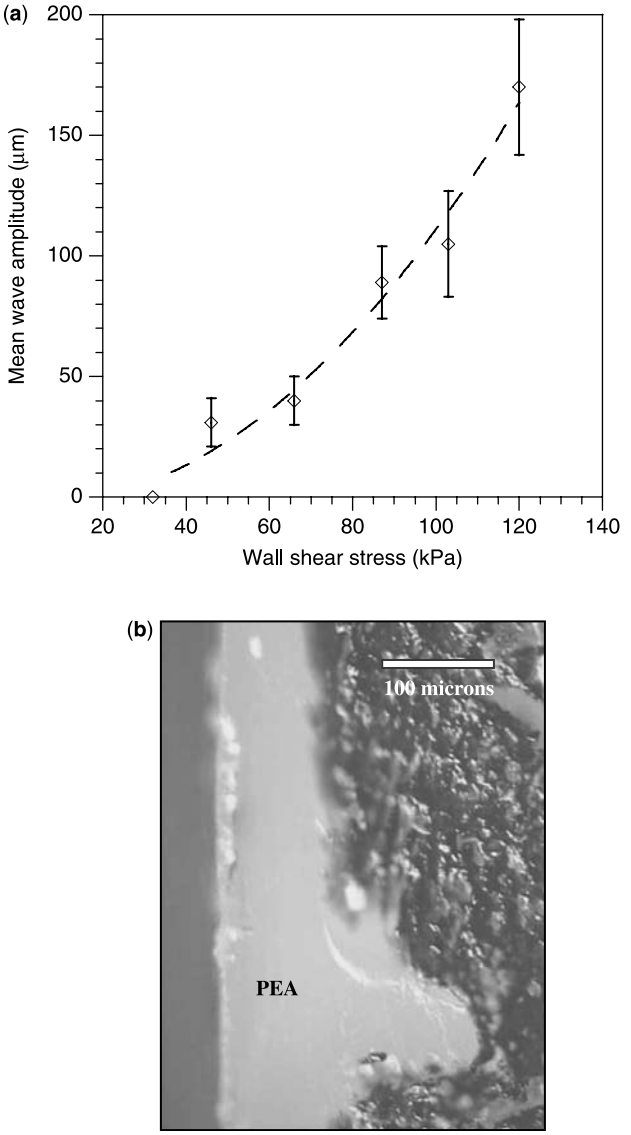

Fig. 18-9 (a) Mean wave amplitude as a function of shear stress; (b) illustration of the mechanical interlocking and wave amplitude for PEA/PLS2/PEA films. Source: Martin and Avérous (2002).

18.4.2 Coextrusion Analysis of the Solid-State Behavior

This section is more particularly focused on the analysis of the coextruded materials after cooling. The behavior of several polyesters has been tested in association with different PLS formulations.

Adhesion Strength Between PLS and Biopolyester Layers Figure 18-10 shows peel strength results of coextruded films, based on PLS3 and different polyesters. The polyester amide (PEA) is seen to have the highest peel strength, which is linked to its polar nature; PBSA and PCL have medium values; and PLA and PHBV have the lowest ones. Although peel strength does not constitute an absolute measure of adhesion, it reflects the compatibility or affinity between PLS and the respective polyesters. This result confirms well some previous findings on the compatibility of plasticized starch with polyesters (Avérous, 2004) through the study of blended systems. These results are in good agreement with those of Biresaw and Carriere (2000) or, more recently, with those of Schwach and Avérous (2004).

It is well known that plasticizers migrating toward the surface of polymers can significantly affect the adhesion. The amount of plasticizer (water, glycerol) added to starch for processing purposes is likely to affect the adhesion strength between the layers of plasticized starch–polyester structures. We have previously reported the tendency of highly plasticized starch to exude toward the surface with time (Avérous et al., 2000a). Table 18-6 presents the peel strength data of PLS/polyester coextruded structures, with different PLS formulations as the central layer, and with various biopolyesters as the outer layers. From Table 18-6 it is obvious that the peel strength decreases as the glycerol/starch (G/S) ratio increases. For instance, the peel strength of PLS/PLA laminates ranges from 0.12 to 0.05 N/mm for G/S ratio comprised between 0.14 and 0.54. These results seem to show that polyol migration to the interface occurs readily, whatever the polyester skin layer. This is in agreement with the results of Wang et al. (2000). However, the multilayers prepared with PLS pellets (conditions 7 to 10, Table 18-6) did not show the same trend, in that the peel strength data lie around 0.2 N/mm while the G/S ratio varied from 0.14 to 0.50. This result could be interpreted in terms of the diminution of the water content after extrusion and equilibration of the PLS granules (Table 18-1). We obtained higher polysaccharide–glycerol interactions which are linked to exchanges of

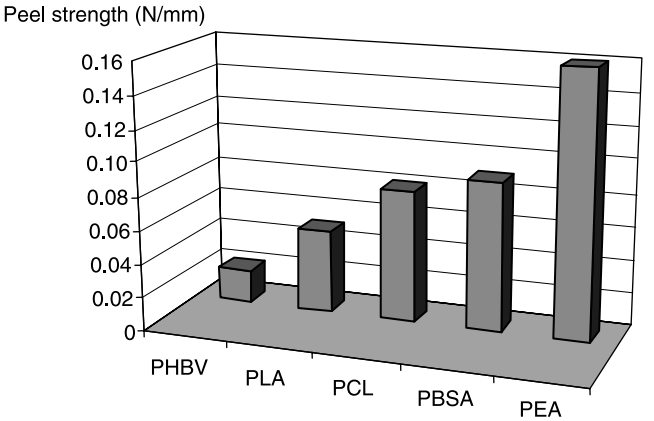

Fig. 18-10 Effect of the type of biopolyester on the peel strength of PLS3-based films.

TABLE 18-6 Effect of PLS Composition on the Peel Strength of Starch–Biopolyester Multilayers[a]

Test No.	Polyester	PLS Type	Film Thickness[b] (μm)	Polyester Layer Thickness[b] (μm)	Peel Strength (N/mm)
1	PEA[c]	PLS1	920	120	0.22 (0.05)[e]
2	PEA	PLS2	910	130	0.18 (0.04)
3	PEA	PLS3	830	120	0.16 (0.03)
4	PLA	PLS1	890	140	0.12 (0.02)
5	PLA[c]	PLS2	900	160	0.11 (0.01)
6	PLA	PLS3	850	140	0.05 (0.01)
7	PEA	PLS1[d]	900	135	0.22 (0.06)
8	PEA[c]	PLS2[d]	880	120	0.24 (0.05)
9	PLA	PLS2[d]	860	115	0.12 (0.04)
10	PEA[c]	PLS3[d]	820	110	0.19 (0.04)

[a]*Source*: Martin et al. (2001).
[b]The thickness was measured at the center, according to the film width.
[c]The multilayer film contained some defects, i.e., instabilities at the interface.
[d]The PLS had previously been extruded and pelletized.
[e]Values between brackets are the standard deviations.

occupation of some strong sites from water to glycerol molecules. This phenomenon induces a decrease of glycerol migrations.

The aging of films is known to influence the peel strength data (Wang et al., 2000). All our tests were performed on 1-week equilibrated (at 23°C, 50% RH) specimens, unless specified otherwise. It was noticed that the adhesion strength varied with time. For instance, the peel strength of PLS/PHBV ranged from slightly adhesive (0.02 N/mm, Fig. 18-10) to nonadhesive, since the PHBV layers spontaneously peeled off the starch layer after 50 weeks. In that case, it was not clearly identified whether the aging, the glycerol migration, or the low compatibility was responsible for the loss of adhesion.

Strategy to Improve Interfacial Adhesion A strategy was tested to improve the adhesion strength between plasticized starch and some biopolyesters. The blended composition was used in the inner starch layer, to enhance the ties between starch and polyester layers. The opposite strategy, adding PLS into the cap layers, must be avoided since the skin layers act as water barriers.

The polyesters constituting the minor phase of blend (i.e., 5 wt% and 10 wt%) were blended with PLS. The influence of a blended PLS inner layer was tested with a selection of three polyesters: PEA, PLA, and PCL. The effects on the peel strength are presented in Fig. 18-11. The dark bars correspond to the peel strength results of coextruded starch-polyester films from Fig. 18-10. The gray and white bars represent the peel strength values of multilayers where the central layers are starch–polyester blends comprising 5% and 10% of polyester, respectively. An increase of 19% to 31% was observed for PEA-based films and 37% to 50% for

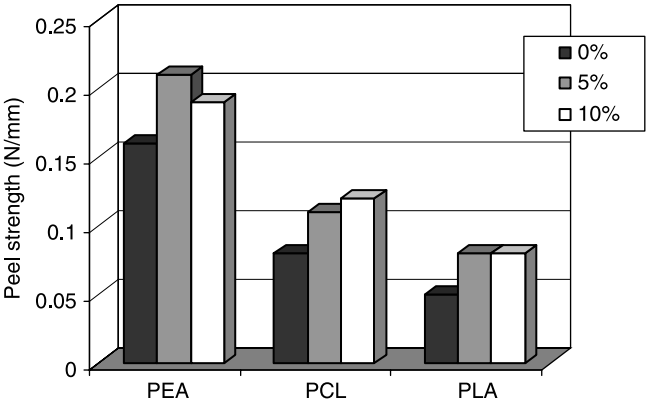

Fig. 18-11 Effect of blend composition (0 wt%, 5 wt%, or 10 wt%) and the type of biopolyester on the peel strength of PLS3/polyester coextruded films. Source: Martin et al. (2001).

PCL-based films, and an increase in peel strength of 40% was observed for PLA-based films. This strategy yielded satisfactory results, although the presence of some defects on the films, referred to as interfacial instabilities (Wang et al., 2000), may partially alter the results. Moreover, these improvements were obtained at the cost of a supplementary operation and use of more polyester, which is not fully desirable from an economic point of view.

Moisture Resistance Properties Figure 18-12 shows the results of contact angle measurements performed on starch–polyester systems, as well as on neat polyesters and plasticized starch. PLS3-blends based on PEA, PLA, and PCL were chosen. Low values of the slope (in absolute value) indicate stronger hydrophobic character of the products. For all blends, it was observed that the hydrophilic character decreased rapidly from 0% to 10% polyester content and kept decreasing until the value of neat biopolyester. PLS/PLA blends, whatever the composition, showed the best characteristics. As expected, better barrier properties can be obtained with starch products laminated with moisture-resistant polyesters, compared with blends. Immersion tests of starch–polyester multilayers in water were also undertaken to check their ability to resist water penetration. Water penetration is known to have detrimental effects on the multilayers, such as the swelling of PLS layers, resulting in the loss of elastic modulus and spontaneous delamination of the cap layers. Over a few days, no significant product swell or delamination was observed. That result is satisfactory since it shows that multilayers have good resistance to moisture. This confirms results of Shogren (1997), who indicated that, although biopolyesters have lower water barrier properties than polyethylene, they can provide sufficient protection to starch products for short-terms applications. Finally, it is interesting to note that the moisture resistance of polyesters (PLA > PCL > PEA) is in inverse order to that of adhesion.

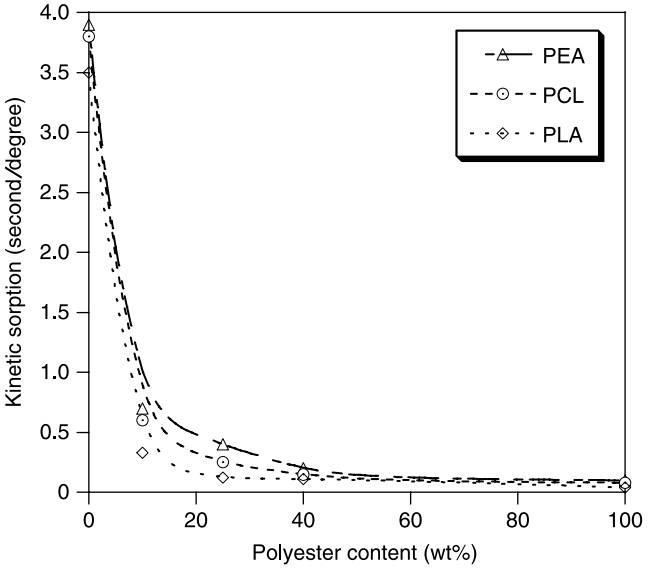

Fig. 18-12 Effect of the polyester content (PEA, PLA, and PCL, % w/w) on the hydrophilic character of the product. Source: Martin et al. (2001).

18.5 CONCLUSION

The development of compostable and low-cost multilayer materials based on plasticized starch and biodegradable polyesters is interesting in more than one sense. One requisite in the preparation of multilayered products based on starch is to obtain sufficient adhesion between layers, moisture barrier properties, and uniform layer thickness distribution.

Experimental results on melt-state during the process show that the key parameters are the skin-layer viscosity and thickness, the global extrusion rate, and the die geometry. Under certain conditions, reasonable layer uniformity was obtained across the wide die width, and encapsulation of the central starch layer at both edges of the die could not be avoided, even when the cap layers were the highest viscosity component. However, side wall encapsulation is not thought to be very critical. Closer attention should be given to the interfacial instabilities since they may be more detrimental to the coextruded material and final product. The occurrence of instabilities is strongly related to the shear stress at the interface. Flow conditions ranging from stable to unstable can be obtained. Investigation of the flow behavior of starch/PEA multilayers allows us to classify the instabilities according to the dominating factors, such as shear stress-, viscosity difference-, or melt stream confluence point-driven instabilities. The interfacial instability amplitude of multilayer films can be controlled through the wall shear stress. Under control, these instabilities can generate mechanical interlocking and thus increase the interfacial adhesion strength of the coextruded material.

Experimental results on coextruded materials show that different levels of peel strength can be found, depending on the compatibility of plasticized starch with the respective biopolyesters. In particular, poly(ester amide) (PEA) presents the highest adhesion with the PLS layer, probably due to its polar amide groups. PCL and PBSA showed medium adhesion values, and PLA or PHBV were the less-compatible polyesters. However, it was possible to increase the adhesion properties of the film by up to 50%, by introducing polyester blends in the central layer. We show that the different multilayers exhibit satisfactory water resistance properties.

The use of the coextrusion technique is validated for preparation of compostable multilayer films based on plasticized starch for such uses as short-term packaging. Nevertheless, the scope of these investigations is limited on one hand by the narrow processing range of PLS products and, on the other, by the lack of viscoelastic data for low-moisture starch melts. In many cases, elastic properties of polymer melts are equally important in the mechanism of interfacial instabilities.

There are some inherent problems due to the multilayer flow conditions encountered in coextrusion, such as the phenomena of encapsulation and interfacial instabilities. It is crucial to address these problems because they can be detrimental to the product, affecting quality and functionality.

ACKNOWLEDGMENTS

This work was funded by Europol'Agro (Reims, France) through a research program devoted to the study and development of new packaging materials based on renewable resources. The authors thank Dr. Olivier Martin and Dr. Emmanuelle Schwach for their inputs into these studies.

REFERENCES

Amass W, Amass A, Tighe B. 1998. A review of biodegradable polymers: uses, current developments in the synthesis and characterization of biodegradable polyesters, blends of biodegradable polymers and recent advances in biodegradation studies. *Polym Int* 47:89–144.

Avérous L. 2004. Biodegradable multiphase systems based on plasticized starch: a review. *J Macomol Sci Part C Polym Rev* C4:231–274.

Avérous L, Fringant C. 2001. Association between plasticized starch and polyesters: processing and performances of injected biodegradable systems. *Polym Eng Sci* 41:727–734.

Avérous L, Fringant C, Martin O. 1999. Coextrusion of biodegradable starch-based materials. In: *Biopolymer Science: Food and Non-Food Applications*. Colonna P, Guilbert S, editors. Paris: INRA. p. 207–212.

Avérous L, Fauconnier N, Moro L, Fringant C. 2000a. Blends of thermoplastic starch and polyesteramide: processing and properties. *J Appl Polym Sci* 76:1117–1128.

Avérous L, Moro L, Dole P, Fringant C. 2000b. Properties of thermoplastic blends: starch-polycaprolactone. *Polymer* 41:4157–4167.

Bastioli C, Cerutti A, Guanella I, Romano GC, Tosin M. 1995. Physical state and biodegradation behavior of starch–polycaprolactone systems. *J Environ Polym Degrad* 3:81–95.

Belard L, Dole P, Avérous L. 2005. Current progress on biodegradable materials, based on plasticized starch. *Aust J Chem* 58:457–460.

Biresaw G, Carriere CJ. 2000. Interfacial properties of starch/biodegradable esters blends. *Polymer preprints* 41:64–65.

Dooley J. 2005. Co-extrusion instabilities. In: *Polymer Processing Instabilities: Control and Understanding*. Hatzikiriakos S, Migler K, editors. New York: CRC Press. p. 383–426.

Dooley J, Stout B. 1991. An experimental study of the factors affecting the layer thickness uniformity of coextruded structures. *Soc Plast Eng Annu Tech Meet* 37:62–65.

Dooley J, Hyun KS, Hugues K. 1998. An experimental study on the effect of polymer viscoelasticity on layer rearangement in coextruded structures. *Polym Eng Sci* 38:1060–1071.

Gifford WA. 1997. A three dimensional analysis of coextrusion. *Polym Eng Sci* 37:315–320.

Han CD. 1981. *Multiphase Flow in Polymer Processing*. New York: Academic Press.

Han CD, Shetty R. 1976. Studies on multilayer film coextrusion I The rheology of flat film coextrusion. *Polym Eng Sci* 16:697–705.

Han CD, Shetty R. 1978. Studies on multilayer film coextrusion II. Interfacial instability in flat film coextrusion. *Polym Eng Sci* 18:180–186.

He Y, Asakawa N, Masuda T, Cao A, Yoshie N, Inoue Y. 2000. The miscibility and biodegradability of poly3-hydroxybutyrate blends with polybutylene succinate-*co*-butylene adipate and polybutylene succinate-*co*-caprolactone. *Eur Polym J* 36:2221–2229.

Hickox CE. 1971. Instability due to viscosity stratification in axisymmetric pipe flow. *Phys Fluids* 14:251–262.

Huang SJ, Koening MF, Huang M. 1993. Design, synthesis, and properties of biodegradable composites. In: *Biodegradable Polymers and Packaging*. Ching C, Kaplan DL, Thomas EL, editors. Basel: Technomic Publication. p. 97–110.

Hulleman SHD, Janssen FHP, Feil H. 1998. The role of water during plasticization of native starches. *Polymer* 39:2043–2048.

Hulleman SHD, Kalisvaart MG, Janssen FHP, Feil H, Vliegenthart JFG. 1999. Origins of B-type crystallinity in glycerol-plasticised compression-moulded potato starches. *Carbohydr Polym* 39:351–360.

Huneault M, Li H, 2007. Morphology and properties of compatibilized polylactide/thermoplastic starch blends. *Polymer* 48:270–280.

Karagiannis A, Mavridis H, Hrymak AN, Vlachopoulos J. 1988. Interface determination in bicomponent extrusion. *Polym Eng Sci* 28:982–988.

Khan AA, Han CD. 1976. On the interface deformation in the stratified two-phase flow of viscoelastic fluids. *Trans Soc Rheol* 20:595–621.

Khomani B. 1990a. Interfacial instability and deformation of two stratified power law fluids in plane poiseuille flow 1 Stability analysis. *J Non-Newton Fluid Mech* 36:289–303.

Khomani B. 1990b. Interfacial instability and deformation of two stratified power law fluids in plane poiseuille flow 2 Interface deformation. *J Non-Newton Fluid Mech* 37:19–36.

Koenig MF, Huang SJ. 1995. Biodegradable blends and composites of polycaprolactone and starch derivatives. *Polymer* 36:1877–1882.

Krook M, Morgan G, Hedenqvist MS. 2005. Barrier and mechanical properties of injection molded montmorillonite/polyesteramide nanocomposites. *Polym Eng Sci* 45:135–141.

Lawton JW. 1997. Biodegradable coatings for thermoplastics starch. In: *Cereals: Novel Uses and Process*. Campbell GM, Webb C, McKee SL, editors. New York: Campbell Plenum Press. p. 43–47.

Lee BL, White JL. 1974. An experimental study of rheological properties of polymer melts in laminar shear flow and of interface deformation and its mechanisms in two-phase stratified flow. *Trans Soc Rheol* 18:467–492.

Martin O, Avérous L. 2001. Polylactic acid: plasticization and properties of biodegradable multiphase systems. *Polymer* 42:6209–6219.

Martin O, Avérous L. 2002. Comprehensive experimental study of a starch/polyesteramide coextrusion. *J Appl Polym Sci* 86:2586–2600.

Martin O, Schwach E, Avérous L, Couturier Y. 2001. Properties of biodegradable multilayer films based on plasticized wheat starch. *Starch/Staerke* 37:372–380.

Martin O, Avérous L, Della Valle G. 2003. Inline determination of plasticized wheat starch viscous behaviour: Impact of processing. *Carbohydr Polym* 53:169–182.

Matzinos P, Tserki V, Kontoyiannis A, Panayiotou C. 2002. Processing and characterization of starch/polycaprolactone products. *Polym Degrad Stab* 77:17–24.

Mavradis H, Schroff R. 1994. Multilayer extrusion: Experiments and computer simulation. *Polym Eng Sci* 34:559–569.

Mitsoulis E. 1988. Multilayer sheet coextrusion: analysis and design. *Adv Polym Tech* 8:225–242.

Myllymäki O, Myllärinen P, Forssell P, et al. 1998. Mechanical and permeability properties of biodegradable extruded starch/polycaprolactone films. *Pack Technol Sci* 11:265–274.

Narayan R, Krishnan M. 1995. Biodegradable composites and blends of starch with polycaprolactone. *Polym Mater Sci Eng* 72:186–187.

Perdikoulias J, Richard C, Vlcek J, Vlachopoulos J. 1991. A study of coextrusion flows in polymer processing. In: ANTEC Proceedings, SPE (Society of Plastics Engineers), Montreal, p. 2461–2464.

Pranamuda H, Tokiwa Y, Tanaka H. 1996. Physical properties and biodegradability of blends containing polycaprolactone and tropical starches, *J Environ Polym Degrad* 4:1–7.

Ramsay BA, Langlade V, Carreau PJ, Ramsay JA. 1993. Biodegradability and mechanical properties of polyhydroxybutyrate-*co*-hydroxyvalerate–starch blends. *Appl Environ Microbiol* 59:242–1246.

Ranjbaran MM, Khomani B. 1996. The effect of interfacial instability on the strength of the interface in two-layer plastic structures. *Polym Eng Sci* 36:1875–1885.

Ratto JA, Stenhouse PJ, Auerbach M, Mitchell J, Farrell R. 1999. Processing, performance and biodegradability of a thermoplastic aliphatic polyester/starch system. *Polymer* 40:6777–6788.

Rouilly A, Rigal L. 2002. Agro-materials: a bibliographic review. *J Macromol Sci Part C Polym Rev* 4:441–479.

Schrenck WJ, Alfrey T Jr. 1978. Coextruded multilayer films and sheets, In: *Polymer Blends*, Volume 2. Paul DR, Newman S, editors. London: Academic Press. p. 129–165.

Schrenck WJ, Bradley NL, Alfrey T Jr, Maack H. 1978. Interfacial flow instability in multilayer coextrusion. *Polym Eng Sci* 18:620–623.

Schwach E, Avérous L. 2004 Starch-based biodegradable blends: morphology and interface properties. *Polym Int* 53:2115–2124.

Shogren RL. 1997. Water vapor permeability of biodegradable polymers. *J Environ Polym Degrad* 5:91–95.

Shogren RL, Lawton JW. 1998. Enhanced water resistance of starch-based materials. US Patent 5,756,194.

Sornberger G, Vergnes B, Agassant JF. 1986a. Coextrusion of two molten polymers between parallel plates: non-isothermal computation and experimental study. *Polym Eng Sci* 26:682–689.

Sornberger G, Vergnes B, Agassant JF. 1986b. Two directional coextrusion flow of two molten polymers in flat dies. *Polym Eng Sci* 26:455–460.

Southern JH, Ballman RL. 1973. Stratified bicomponent flow of polymer melts in a tube. *J Appl Polym Sci* 20:175–189.

Steinbuchel A. 2003. *Biopolymers, General Aspects and Special Applications*. Weinheim: Wiley-VCH.

Su YY, Khomani B. 1992a. Purely elastic interfacial instabilities in superposed flow of polymeric fluids. *Rheol Acta* 31:413–420.

Su YY, Khomani B. 1992b. Interfacial stability of multilayer viscoelastic fluids in slit and converging channel die geometries *J Rheol* 36:357–387.

Swanson CL, Shogren RL, Fanta GF, Imam SH. 1993. Starch–plastic materials—preparation, physical properties, and biodegradability. *J Environ Polym Degrad* 1:155–166.

Tomka I. 1991. Thermoplastic starch. *Adv Exp Med Biol* 302:627–637.

Tzoganakis C, Perdikoulias J. 2000. Interfacial instabilites in coextrusion flows of low-density polyethylenes: Experimental studies. *Polym Eng Sci* 40:1056–1064.

Van de Velde K, Kiekens P. 2002. Biopolymers: overview of several properties and consequences on their applications. *Polym Test* 21:433–442.

Van Soest JJG, Hulleman SHD, De Wit D, Vliegenthart JFG. 1996. Crystallinity in starch plastics. *Ind Crops Prod* 5:11–22.

Van Tuil R, Schennink G, De Beukelaer H, Van Heemst J, Jaeger R. 2000. Converting biobased polymers into food packaging. In: Claus J, Weber, editor. *The Food Biopack Conference*. Proceedings of the meeting held in Copenhagen, Denmark, August 2000. The Royal Veterinary and Agricultural University, Denmark. p. 28–30.

Verhoogt H, St-Pierre N, Truchon FS, Ramsay BA, Favis BD, Ramsay JA. 1995. Blends containing polyhydroxybutyrate-*co*-12%-hydroxyvalerate and thermoplastic starch. *Can J Microbiol* 41:323–328.

Vikman M, Hulleman SHD, Van Der Zee M, Myllarinen P, Feil H. 1999. Morphology and enzymatic degradation of thermoplastic starch–polycaprolactone blends. *J Appl Polym Sci* 74:2494–2604.

Wang L, Shogren RL, Carriere C. 2000. Preparation and properties of thermoplastic starch-polyester laminate sheets by coextrusion. *Polym Eng Sci* 40:499–506.

White JL, Ufford RC, Dharod KR, Price RL. 1972. Experimental and theoritical study of the coextrusion of two-phase molten polymer systems. *J Appl Polym Sci* 16:1313–1330.

Wilson GM, Khomani B. 1992. An experimental investigation of interfacial instabilities in multilayer flow of viscoelastic fluids 1 Incompatible polymer systems. *J Non-Newton Fluid Mech* 45:355–384.

Wilson GM, Khomani B. 1993. An experimental investigation of interfacial instabilities in multilayer flow of viscoelastic fluids. 2. Elastic and non-linear effects in incompatible polymer systems. *J Rheol* 37:315–339.

Yih CS. 1967. Instability due to viscosity stratification. *J Fluid Mech* 27:337–352.